

**$^8\text{Be}$  producing reactions in  $^{12}\text{C} + ^{12}\text{C}$ ,  $^{16}\text{O} + ^{16}\text{O}$ , and  $^{28}\text{Si} + ^{12}\text{C}$ <sup>†</sup>**

J. L. Artz,\* M. B. Greenfield,† and N. R. Fletcher

*Department of Physics, The Florida State University, Tallahassee, Florida 32306*

(Received 2 June 1975)

The  $^{12}\text{C}(^{12}\text{C}, ^8\text{Be})$ ,  $^{16}\text{O}(^{16}\text{O}, ^8\text{Be})$ , and  $^{28}\text{Si}(^{12}\text{C}, ^8\text{Be})$  reactions show final state relative populations which are very similar to the corresponding ( $^6\text{Li}, d$ ), ( $^7\text{Li}, t$ ), ( $^{12}\text{C}, \alpha$ ), and ( $^{16}\text{O}, ^{12}\text{C}$ ) reactions on the same target nuclei. Selective population of final states for  $^{12}\text{C}$  and  $^{28}\text{Si}$  targets is accompanied by rapidly fluctuating excitation functions for the  $^{12}\text{C}(^{12}\text{C}, ^8\text{Be})$  reactions and much smoother, yet not flat, excitation functions for  $^{28}\text{Si}(^{12}\text{C}, ^8\text{Be})$ . Angular distributions are forward peaked. The  $^{16}\text{O}(^{16}\text{O}, ^8\text{Be})$  reaction is not selective, similar to  $^{16}\text{O}(^{12}\text{C}, \alpha)$ .

[ NUCLEAR REACTIONS  $^{12}\text{C}(^{12}\text{C}, ^8\text{Be})^{16}\text{O}^*$ , measured excitation functions  $E_{c.m.}$  = 17 to 21 MeV,  $\sigma(\theta)$  at 21 MeV;  $^{16}\text{O}(^{16}\text{O}, ^8\text{Be})^{24}\text{Mg}^*$ ;  $^{28}\text{Si}(^{12}\text{C}, ^8\text{Be})^{32}\text{S}^*$ , measured excitation functions  $E_{c.m.}$  = 23 to 29 MeV,  $\sigma(\theta)$  at 29.4 MeV. ]

## I. INTRODUCTION

The use of heavy ion induced reactions to investigate cluster structures in nuclei has been an area of considerable interest and activity.<sup>1,2</sup> In most cases the dominant mechanism for the reactions used to investigate these structures (four- and eight-particle transfer reactions) has not been firmly established. The existing experimental results have not been definitive in establishing consistency for either four- or eight-particle transfer reactions with different projectiles and targets. In many cases, a single piece of experimental data might strongly suggest a dominant reaction mode, but when one examines the observables collectively (energy dependence, angular distributions, and selectivity) existing interpretations have not been satisfactory.

The  $^{12}\text{C}(^6\text{Li}, d)^{16}\text{O}$  reaction<sup>3,4</sup> and the  $^{12}\text{C}(^7\text{Li}, t)^{16}\text{O}$  reaction<sup>3,5</sup> have been found to exhibit some selectivity for exciting particular states in  $^{16}\text{O}$ , although the reaction mechanism is not clear. Selectivity implies that a particular reaction will populate some states in the residual nucleus considerably more than other states of the same  $J^\pi$  at approximately the same excitation energy. The above reactions selectively excite states of a four-particle and four-hole (4p-4h) character with regard to the closed shell model core of  $^{16}\text{O}$ , namely those states with excitation energy and spin parity of 6.06 MeV ( $0^+$ ), 6.93 ( $2^+$ ), 10.34 ( $4^+$ ), and 16.3 ( $6^+$ ). Recent analysis of four-particle transfer reactions leading to low-lying states of  $^{28}\text{Si}$  indicates a direct transfer.<sup>6</sup> This result offers some hope that for targets with  $A \geq 24$  the four-particle transfer reactions might be more direct in nature than they are for lighter target. Four-particle transfer reactions measured for  $^{28}\text{Si}$  targets<sup>9-11</sup> show some

selectivity, but detailed analyses of these results have not been presented.

In contrast to the four-particle transfer reaction, the eight-particle transfer reaction  $^{16}\text{O}(^{12}\text{C}, \alpha)^{24}\text{Mg}$  does not selectively populate<sup>6</sup> the ground state rotational band of  $^{24}\text{Mg}$  which has been suggested to have an 8p-0h character.<sup>7</sup> This reaction has been interpreted as proceeding by a compound nucleus reaction mechanism following a statistical analysis of the fluctuating excitation functions.<sup>6</sup>

The present work reports results of an initial survey of some reactions involving either four-nucleon or eight-nucleon transfer in which the  $^8\text{Be}$  ground state is detected in the exit channel. These reactions are compared with the corresponding reactions induced by beams of  $^6\text{Li}$ ,  $^7\text{Li}$ ,  $^{12}\text{C}$ , and  $^{16}\text{O}$  particles. An attempt is made to evaluate the role which these reactions play in the elucidation of  $\alpha$ -particle structures in the residual nuclei.

II.  $^8\text{Be}$  DETECTION

The  $^8\text{Be}$  reaction products are detected following the bombardment of thin self-supporting foils of  $\text{SiO}_2$  or carbon with beams of 20 to 50 particle nA of oxygen and carbon produced by the Florida State University S-FN Tandem Van de Graaff. The targets flashed with about  $10 \mu\text{g}/\text{cm}^2$  of Au were fabricated and handled such as to produce a minimum of impurity buildup. The target thickness and beam intensity were monitored continuously by observing the  $90^\circ$  elastic scattering with a surface barrier detector.

## A. Kinematics, detectors, and circuitry

The  $^8\text{Be}$  particles are identified by the coincidence detection of the two  $\alpha$  particles from the

decay of  ${}^8\text{Be}$ . The high velocity  ${}^8\text{Be}$  nucleus undergoes an isotropic decay from its zero spin ground state while in flight. Because of the low breakup energy, the decay  $\alpha$  particles are confined within a cone with half angle  $\beta$  measured from the  ${}^8\text{Be}$  velocity vector, given by the equation  $\sin\beta = (\epsilon/E_B)^{1/2}$ , where  $\epsilon = 92$  keV and  $E_B$  is the  ${}^8\text{Be}$  energy. For  $E_B \sim 40$  MeV, we have  $\beta \sim 3^\circ$  and, therefore, to maximize detection efficiency the detectors should span most of the cone projection and be very closely spaced.

The detectors, fabricated by ORTEC, are silicon surface barrier detectors with  $200\text{ mm}^2$ , are  $300\text{ }\mu\text{m}$  in depletion depth, and have a  $1\text{ mm}$  dead strip along a diameter separating two electrically independent halves of the detector. Two such detector pairs were mounted in a  $45\text{ cm}$  diameter scattering chamber. Nickel or aluminum foils were placed in front of the detectors to absorb the elastically scattered  ${}^{16}\text{O}$  or  ${}^{12}\text{C}$  particles, thereby reducing the accidental coincidence rate and extending detector life.

A block diagram of the electronics used is shown in Fig. 1. Constant fraction trigger (CFT) circuits were used to derive the timing information inputs to the time-to-amplitude converter (TAC), the output of which is stored as the ungated time spectrum in an analog-to-digital converter (ADC). The coincidence peak in the time spectrum passes through a  $20\text{ nsec}$  window of a timing single channel analyzer (TSCA) and forms the prompt coincidence time spectrum designating valid  ${}^8\text{Be}$  events. The energy information of the  $\alpha$  particles detected in coincidence is gated by the same TSCA

output. These analog energy signals are summed and stored as the  ${}^8\text{Be}$  energy spectrum.

#### B. Detection efficiency

A Monte Carlo computer code has been used to calculate the  ${}^8\text{Be}$  detection efficiency and the effective solid angle of the split detector as a function of  ${}^8\text{Be}$  energy  $E_B$  and a number of geometric parameters. The half-life of  ${}^8\text{Be}$  is sufficiently short that the decay occurs within a few hundred angstroms of its formation site, and that distance may be neglected in the calculation. The probability that a  ${}^8\text{Be}$  particle directed towards a unit area of detector surface leads to a valid event is calculated by first choosing the unit area position then randomly selecting two angles defining the  ${}^8\text{Be}$  breakup axis, thereby fixing the velocity vector directions of the decay  $\alpha$  particles. The event is stored as a valid one if the resulting positions of the  $\alpha$ -particle trajectories, as projected onto the detector, occur one each within the geometric confines of the two halves of the detecting surface. After a large number of possible breakup axes have been randomly chosen, the ratio of valid events to total events is stored as the relative  ${}^8\text{Be}$  detection efficiency for that small unit area of the detector. A display of the results of such a calculation over a gridded quadrant of the detector is shown in Fig. 2. The representative calculation is for a circular detector of radius  $\rho$  of  $0.8\text{ cm}$ , a distance from the target  $D$  of  $12.5\text{ cm}$ , and a dead strip width of  $0.1\text{ cm}$ . Near the center of the detector the  ${}^8\text{Be}$  detection efficiency exceeds  $90\%$ .

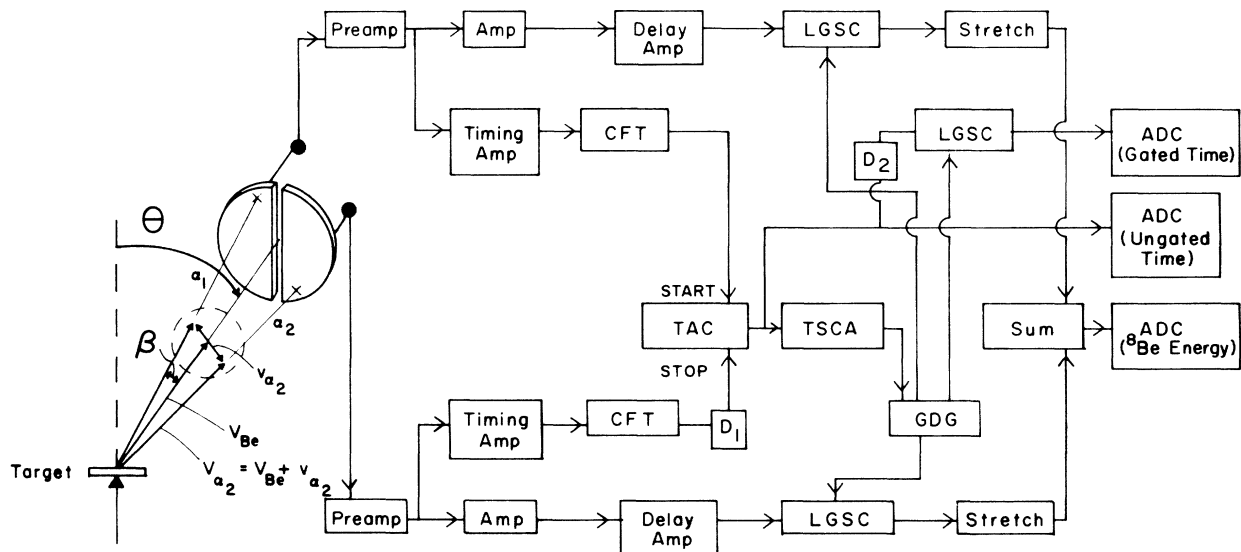


FIG. 1. Block diagram of the electronics used in  $\alpha$ - $\alpha$  coincidence detection of  ${}^8\text{Be}$ .

For these parameters the detection efficiency averaged over the entire surface is about 15%. With 15% average efficiency over the total solid angle subtended, the effective solid angle is  $\sim 2$  msr. Although this effective solid angle could be made much larger by decreasing the value of  $D$ , the angular width of the efficiency curve increases correspondingly. The distance used in this work of 12.5 cm represents a compromise value.

The dependence of the effective solid angle calculation on the parameters was checked experimentally by repeating cross section measurements for different values of  $D$ ,  $\rho$ , and  $E_B$ . The energy dependence was checked by measuring the  $^{12}\text{C}-(\alpha, ^8\text{Be})^8\text{Be}$  cross section at complementary angles in the center of mass where the  $^8\text{Be}$  yield must be symmetric about  $\theta_{\text{c.m.}} = 90^\circ$ , even though the  $^8\text{Be}$  energies measured in the laboratory are drastically different.<sup>12</sup> These measurements were consistent with the calculations within expected statistical errors.

### C. Advantages and disadvantages

The investigation of reactions involving the detection of  $^8\text{Be}$  particles has a number of advantages and disadvantages when compared with similar transfer reactions emitting other heavy ions. With the simple  $\alpha$ -particle coincidence method, the following advantages are provided:

- (a) The coincidence requirement provides a straightforward method of eliminating other competing two-body reaction products. There is no problem with isotopic identification such as is present with counter telescopes which do not employ time of flight.
- (b) The ambiguity, present in most heavy ion re-

actions, of detecting a particle in an excited state is greatly reduced for a number of reasons. The large breakup cone for  $^8\text{Be}^*$  results in a detection efficiency which is only a few percent of that for  $^8\text{Be}$  ground state. In addition, the threshold energy for  $\alpha$ -particle detection was set such that one of the  $\alpha$  particles from  $^8\text{Be}^*$  had insufficient energy to trigger the coincidence timing circuitry. (c) Stopping foils may be used in front of the detectors to absorb both elastically scattered heavy ions and other heavy ion reaction products, since the particles actually detected are light ions. This leads to longer detector life and the possibility of measuring cross sections through  $0^\circ$ .<sup>13,14</sup> (d) The present system is much simpler than the split  $\Delta E$  detector counter telescope<sup>15</sup> for detection of  $^8\text{Be}$  particles. This simplicity has resulted in extensions of the method to multiangle  $^8\text{Be}$  detection systems.<sup>16</sup>

Disadvantages of the present system would include the following. One is unable to observe the energy spectra of  $^8\text{Be}^*$  particles as is done when the energy of each  $\alpha$  particle is recorded on-line.<sup>16</sup> The absorber foil produces energy straggling which in the present work degrades the energy resolution by  $\sim 200$  keV. A large inherent kinematic spread is associated with the large detection efficiency, due to the decay cone geometry. This effect could be greatly reduced in the coincident position sensitive detector method of Scheibling.<sup>17</sup> Experiments involving  $^8\text{Be}$  reaction products do not lend themselves to conventional high resolution techniques, again due to the geometry of the breakup cone.

## III. RESULTS AND DISCUSSION

### A. $^{12}\text{C}(^{12}\text{C}, ^8\text{Be})^{16}\text{O}^*$ reaction

A typical energy spectrum of  $^8\text{Be}$  particles observed from the  $^{12}\text{C}(^{12}\text{C}, ^8\text{Be})^{16}\text{O}^*$  reactions is shown in Fig. 3. The states of  $4p-4h$  structure appear to be strongly populated, very similar to a spectrum reported earlier.<sup>15</sup> Other states populated but rather weakly by this reaction at this energy are the 11.10 MeV ( $4^+$ ) state and the ground state. No noticeable strength is shown to members of the  $3p-3h$  band. Unfortunately the 6.06 MeV ( $0^+$ ) state is not resolved in this work from the 6.13 ( $3^-$ )  $1p-1h$  state, nor is the 6.92 ( $2^+$ ) state adequately resolved from the 7.12 ( $1^-$ )  $1p-1h$  state. Experimental evidence that the 7.12 ( $1^-$ ) state might also be excited results from the fact that the full width at half-maximum (FWHM) of the 6.92 ( $2^+$ ) peak occasionally exceeds the FWHM of the 6.06 ( $0^+$ ) peak by as much as 140 keV. Additional support for this possibility comes from  $^{12}\text{C}(^6\text{Li}, d)^{16}\text{O}$  and  $^{12}\text{C}(^7\text{Li}, t)^{16}\text{O}$  spectra,<sup>4-5</sup> where the 7.12

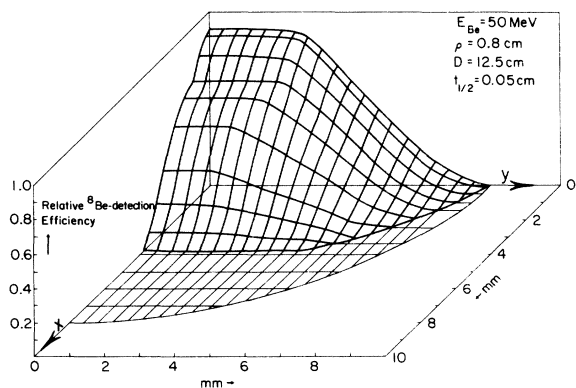


FIG. 2. Detection efficiency per unit area shown over one quadrant of the surface of the split detector. The dividing dead strip is along the  $y$  axis and has a half-width  $t_{1/2}$ . The collimation radius is  $\rho$  and  $D$  is the target to detector distance.

MeV state is resolved, and it is found to be populated although only with  $\sim 10\%$  of the strength of the 6.92 ( $2^+$ ) state. Some earlier work on lithium induced reactions<sup>3</sup> with better energy resolution ( $\sim 40$  keV) shows similar results for the 7 MeV doublet, but actually much stronger excitation of the 6.13 MeV ( $3^-$ ), 1p-1h state, than for the 6.06 MeV ( $0^+$ ), 4p-4h state. In the spectrum of Fig. 3, as in all spectra in the present work, the relative yields for states within these two doublets cannot be determined; however, for purposes of identification, they will be referred to as the 6.06 ( $0^+$ ) and 6.92 ( $2^+$ ), 4p-4h states.

The results of spectra for  ${}^{12}\text{C}({}^{12}\text{C}, {}^8\text{Be}){}^{16}\text{O}$  may be compared with spectra from other four-particle transfer reactions. For example, the  ${}^{12}\text{C}({}^{16}\text{O}, {}^{12}\text{C}){}^{16}\text{O}^*$  reactions<sup>18</sup> ( $E_{\text{lab}} = 65$  MeV) also strongly populate the states of 4p-4h structure. Weakly excited at forward angles are the ground state, the 11.10 MeV ( $4^+$ ) state, and the 8.87 ( $2^-$ ) state, which is forbidden by a simple direct transfer of an  $\alpha$  particle. The  ${}^{12}\text{C}({}^7\text{Li}, t){}^{16}\text{O}$  reaction<sup>5</sup> ( $E_{\text{lab}} = 21.1$  MeV) strongly populates the states of 4p-4h structure but also weakly populates the 9.60 ( $1^-$ ) and 11.63 ( $3^-$ ) states, which comprise the beginning of the 3p-3h band, the ground state, the 8.87 ( $2^-$ ) state, the 9.85 ( $2^+$ ) state, and many states above 11.6 MeV in excitation energy. The  ${}^{12}\text{C}({}^{20}\text{Ne}, {}^{16}\text{O}){}^{16}\text{O}$  reaction<sup>19</sup> ( $E_{\text{lab}} = 78$  MeV) also shows considerable population of the 4p-4h band but weak population elsewhere. However, the reaction  ${}^{12}\text{C}({}^{10}\text{B}, {}^6\text{Li}){}^{16}\text{O}$  ( $E_{\text{lab}} = 28$  MeV) excited the 8.87 MeV ( $2^-$ ) state as strongly as members of the 2p-2h band.<sup>20</sup> Furthermore, the  ${}^{14}\text{N}(\alpha, d){}^{16}\text{O}$  reaction<sup>21</sup> ( $E_{\text{lab}} = 40$  MeV,  $\theta_{\text{lab}} = 10^\circ$ ) and the  ${}^{13}\text{C}({}^6\text{Li}, t){}^{16}\text{O}$  reaction<sup>22</sup> ( $E_{\text{lab}} = 20$  MeV,  $\theta_{\text{lab}} = 20^\circ$ ) only moderate strength to members of the 4p-4h band while strongly exciting other states. Hence, it appears that the 4p-4h band in

${}^{16}\text{O}$  is populated most strongly when four particles are transferred and when the projectile is an even-even  $N = Z$  nuclei or when it has a strong  $\alpha$ -particle parentage such as  ${}^6\text{Li}$  or  ${}^7\text{Li}$ .

The measured excitation functions for the  ${}^{12}\text{C} - ({}^{12}\text{C}, {}^8\text{Be}){}^{16}\text{O}$  reaction leading to the ground state of  ${}^{16}\text{O}$  and  $J^\pi = 0^+$ ,  $2^+$ , and  $4^+$  members of the 4p-4h band of  ${}^{16}\text{O}$  are shown in Fig. 4 for reaction angles of  $\theta_{\text{lab}} = 5^\circ$  and  $25^\circ$ . These yield curves show fluctuations varying from 0.2 to 1.5 MeV in width although the ground state yield appears to flatten above 21 MeV. The energy increments for the present data were not sufficiently small to demonstrate clearly intermediate structure or to allow one to perform a fluctuation analysis. However, the gross fluctuation widths observed here compare with those observed in the  ${}^{12}\text{C} + {}^{12}\text{C}$  elastic scattering.<sup>23</sup> No obvious cross correlations exist between the excitation functions, which may have suggested entrance channel effects. In addition, there is no obvious cross correlation between the two yield curves of Fig. 4 for the same state of  ${}^{16}\text{O}$ , which might suggest resonances in the compound nucleus  ${}^{24}\text{Mg}$ . The maximum near  $E_{\text{c.m.}} = 17.3$  MeV in the  $5^\circ$  yield has been suggested<sup>24</sup> as a component of the  $J^\pi = 10^+$  member of the quasimolecular rotational band. Further investigation with a much more efficient detection system has confirmed this speculative  $J^\pi$  assignment along with identifying many more  $8^+$ ,  $10^+$ , and  $12^+$  states of  ${}^{24}\text{Mg}$ .<sup>25</sup>

The angular distributions for  ${}^{12}\text{C}({}^{12}\text{C}, {}^8\text{Be}){}^{16}\text{O}$  measured at  $E_{\text{c.m.}} = 21.0$  MeV, leading to the ground state of  ${}^{16}\text{O}$  and the  $J^\pi = 0^+$ ,  $2^+$ , and  $4^+$  members of the 4p-4h band are shown in Fig. 5. The ground state has a relatively small and oscillating cross section as compared with the large and relatively smooth cross sections for  $0^+$ ,  $2^+$ , and  $4^+$  members of the 4p-4h band. This same feature is also apparent for the  ${}^{12}\text{C}({}^7\text{Li}, t){}^{16}\text{O}$  reaction,<sup>5</sup> which, supposedly, is predominantly direct at  $E_{\text{lab}} = 21.1$  MeV, although both the ground state and the 4p-4h cross sections are about one order of magnitude less than the cross sections reported in the present work. Any implication regarding a direct mechanism on the basis of the angular distributions of the present work must be qualified by noting the variation of cross section with energy in the vicinity of  $E_{\text{c.m.}} = 21.0$  MeV, observed in the present work and elsewhere.<sup>13, 25, 26</sup> It is clear that if the contribution from the 6.13 MeV ( $1^-$ ) state is small, then quite different mechanisms must account for the cross section observed for the  $0^+$  ground state and the  $0^+$  excited state at 6.06 MeV.

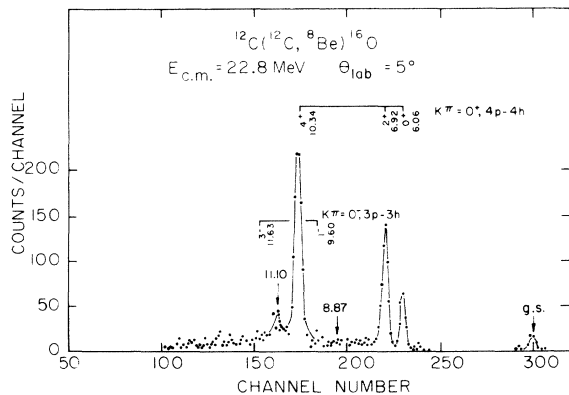


FIG. 3. A typical spectrum for  ${}^{12}\text{C}({}^{12}\text{C}, {}^8\text{Be}){}^{16}\text{O}$  at  $\theta_{\text{lab}} = 5^\circ$  and  $E_{\text{c.m.}} = 22.8$  MeV. Expected positions of residual states with rotational band information are shown.

#### B. ${}^{16}\text{O}({}^{16}\text{O}, {}^8\text{Be}){}^{24}\text{Mg}^*$ reaction

At a bombarding energy of 56 MeV and a  ${}^8\text{Be}$  detection angle of  $5^\circ$  one obtains for  ${}^{16}\text{O}({}^{16}\text{O}, {}^8\text{Be})$

the  $^8\text{Be}$  energy spectrum illustrated in Fig. 6. The effect of  $^{12}\text{C}$  contamination is shown and does not seriously complicate the extraction of cross sections for  $^{24}\text{Mg}$  final states below 7 MeV. The cross sections at  $\theta_{\text{lab}}=5^\circ$  for the  $0^+$  ground state and the  $2^+$  first excited state of  $^{24}\text{Mg}$  at 1.37 MeV are  $8 \pm 2 \mu\text{b/sr}$  and  $120 \pm 10 \mu\text{b/sr}$ , respectively. Strong

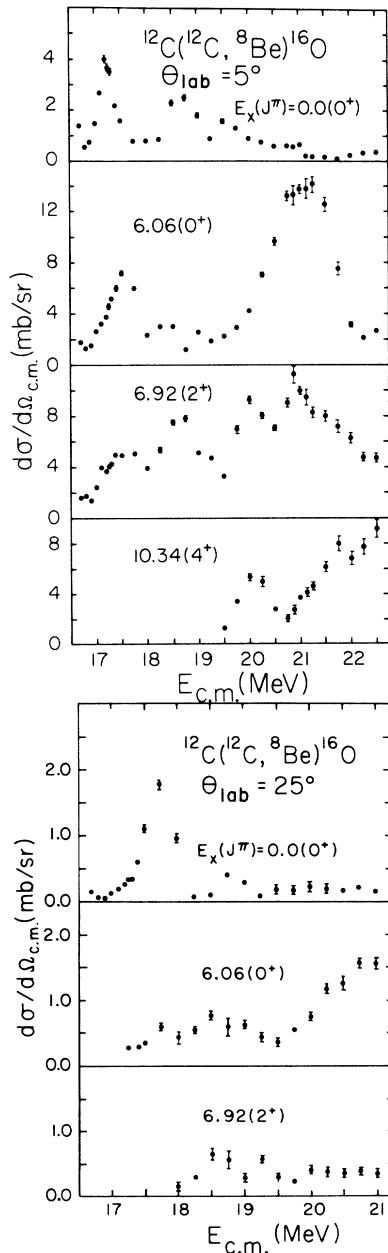


FIG. 4. Excitation functions for  $^{12}\text{C}(^{12}\text{C}, ^8\text{Be})^{16}\text{O}$  measured at  $\theta_{\text{lab}}=5^\circ$  and  $25^\circ$ . The data identified by excitation energies in  $^{16}\text{O}$  of 6.06 and 6.92 MeV may include contributions from the 6.13 and 7.12 MeV states, respectively.

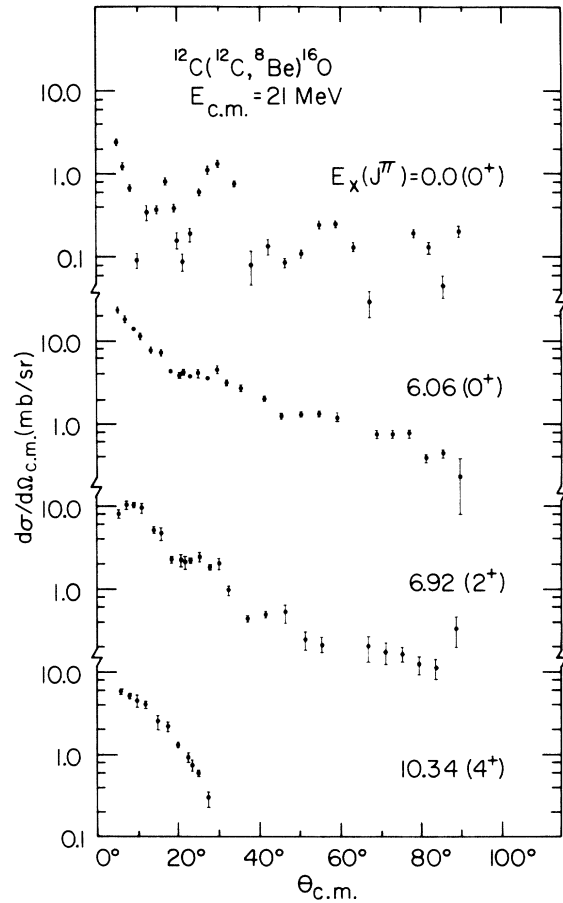


FIG. 5. Angular distributions for  $^{12}\text{C}(^{12}\text{C}, ^8\text{Be})^{16}\text{O}$  at  $E_{\text{c.m.}}=21.0$  MeV. The data identified by excitation energies in  $^{16}\text{O}$  of 6.06 and 6.92 MeV may include contributions from the 6.13 and 7.12 MeV states, respectively.

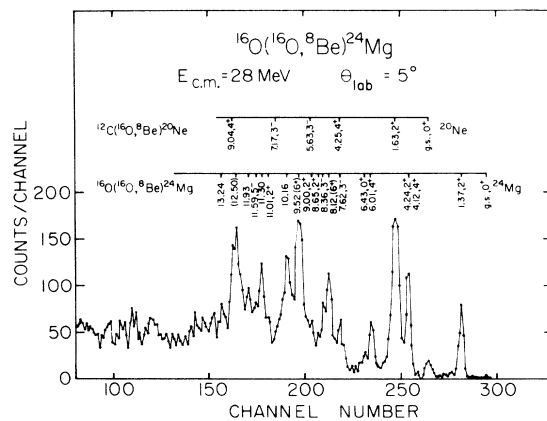


FIG. 6. Energy spectrum of detected  $^8\text{Be}$  particles from  $^{16}\text{O}$  bombardment of  $^{16}\text{O}$ . The states in  $^{24}\text{Mg}$  indicated were identified at five different reaction angles.

states of  ${}^{24}\text{Mg}$  at higher excitation energies are identified in Fig. 6 from an energy calibration curve. These states were identified for each of five laboratory angles at  $E_{\text{lab}} = 56$  MeV. Because of obvious difficulties in resolution and in background subtraction, cross sections for these high-lying states were not extracted in this work.

One fact clearly illustrated in Fig. 6 is that members of the ground state rotational band [0.0 ( $0^+$ ), 1.37 ( $2^+$ ), 4.12 ( $4^+$ ), 8.12 ( $6^+$ ), and 13.18 ( $8^+$ )], suggested as 8p-0h structure, are not preferentially populated in this eight-particle transfer reaction. The general lack of selectivity indicates a dominant nondirect reaction mechanism, no clearly defined 8p-0h<sup>7</sup> structure in  ${}^{24}\text{Mg}$ , or both.

The spectrum of Fig. 6 may be compared with similar spectra also leading to states of  ${}^{24}\text{Mg}$  via the  ${}^{12}\text{C}({}^{16}\text{O}, \alpha){}^{24}\text{Mg}$  reaction<sup>6</sup> in the energy range  $E_{\text{c.m.}} = 19$  to 25 MeV. States strongly populated and identified in the  ${}^{16}\text{O}({}^{16}\text{O}, {}^8\text{Be}){}^{24}\text{Mg}$  spectrum are also found to be strongly populated in the  ${}^{12}\text{C}({}^{16}\text{O}, \alpha){}^{24}\text{Mg}$  reactions. Greenwood *et al.*<sup>6</sup> performed a standard Ericson fluctuation analysis for these states and obtained coherence widths of 90 to 150 keV. Furthermore, the energy averaged cross sections for these states were explained by Hauser-Feshbach statistical-model calculations.

Limited measurements of the angle and energy dependence of cross sections for the low-lying states of  ${}^{24}\text{Mg}$  via the  ${}^{16}\text{O}({}^{16}\text{O}, {}^8\text{Be}){}^{24}\text{Mg}$  reaction were obtained. Because of the very small fluctuating cross sections encountered and the apparent nondirect nature of the  ${}^{16}\text{O}({}^{16}\text{O}, {}^8\text{Be}){}^{24}\text{Mg}$  reaction at this energy, the investigation was terminated.

### C. ${}^{28}\text{Si}({}^{12}\text{C}, {}^8\text{Be}){}^{32}\text{S}$ reaction

The cross sections for  $({}^{12}\text{C}, {}^8\text{Be})$  reactions leading to the ground state of  ${}^{32}\text{S}$  and to excited states of 2.23 MeV ( $2^+$ ) and 5.01 MeV ( $3^-$ ) were extracted from spectra resulting from  ${}^{12}\text{C}$  bombardment of  $\text{SiO}_2$  targets. These spectra are dominated by the yields from  ${}^{16}\text{O}({}^{12}\text{C}, {}^8\text{Be}){}^{20}\text{Ne}^*$  and  ${}^{12}\text{C}({}^{12}\text{C}, {}^8\text{Be}){}^{16}\text{O}^*$  reactions as illustrated in Fig. 7. A spectrum fitting routine was required to extract the areas of  ${}^{32}\text{S}$  peaks. The yield observed near an excitation of 6.75 and 7.4 MeV (not shown in Fig. 7) might correspond to the yield from several unresolved states in  ${}^{32}\text{S}$ .

Four-particle transfer reactions induced by  ${}^6\text{Li}$ ,  ${}^7\text{Li}$ , and  ${}^{16}\text{O}$  ions have also been observed on  ${}^{28}\text{Si}$  targets.<sup>9-11</sup> The  ${}^{28}\text{Si}({}^6\text{Li}, d){}^{32}\text{S}^*$  reaction<sup>9,11</sup> strongly populates the 2.23 MeV ( $2^+$ ) and 5.01 ( $3^-$ ) states of  ${}^{32}\text{S}$ , similar to present work. In addition, there is strong population of the ground state and of states at 4.46 and 5.80 MeV and weaker population of several other states below 6 MeV ex-

citation. The results of Lindgren *et al.*<sup>11</sup> show a large yield at 6.76 and 7.43 MeV excitation, similar to the present work. Some yield for the 5.80 MeV state may be present in the spectrum of Fig. 7 but the yield was not extracted because of the high background present. The  ${}^{28}\text{Si}({}^{16}\text{O}, {}^{12}\text{C}){}^{32}\text{S}$  reaction proceeds most strongly to the excited states at 4.70 and 6.90 MeV. Although no yield was reported for the 5.01 ( $3^-$ ) state,<sup>10</sup> a continuing study<sup>27</sup> indicates that this state dominates the spectrum below 6.5 MeV excitation.

From the results cited the  ${}^{28}\text{Si}({}^{12}\text{C}, {}^8\text{Be}){}^{32}\text{S}$ ,  ${}^{28}\text{Si}({}^6\text{Li}, d){}^{32}\text{S}$ , and  ${}^{28}\text{Si}({}^{16}\text{O}, {}^{12}\text{C}){}^{32}\text{S}$  reactions exhibit marked similarities. The consistently strong population of the 2.23 MeV ( $2^+$ ) and 5.01 MeV ( $3^-$ ) states suggests a direct four-particle transfer component in the reaction mechanism since these reactions proceed through different compound systems. The selective population of the 5.01 MeV ( $3^-$ ) state is especially interesting in light of Arima's [331] quartet prediction at 6.4 MeV of excitation.<sup>28</sup>

Angular distributions at  $E_{\text{c.m.}} = 29.4$  MeV and yield curves at  $\theta_{\text{lab}} = 5^\circ$  and  $25^\circ$  have been obtained for a few final states of the  ${}^{28}\text{Si}({}^{12}\text{C}, {}^8\text{Be}){}^{32}\text{S}$  reaction and are shown in Figs. 8 and 9, respectively. The large relative errors shown are due largely to uncertainties in the peak fitting and background subtraction. Missing points in the angular distributions result from inability to properly resolve two or more peaks. The angular distributions for the ground state and the 2.23 MeV state are very similar in shape to those from the  ${}^{28}\text{Si}({}^{16}\text{O}, {}^{12}\text{C}){}^{32}\text{S}$  re-

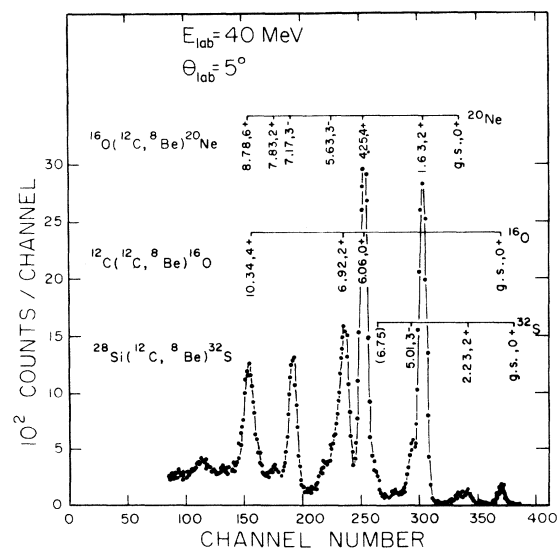


FIG. 7. Energy spectrum of detected  ${}^8\text{Be}$  particles from  ${}^{12}\text{C}$  bombardment of a  $\text{SiO}_2$  target.

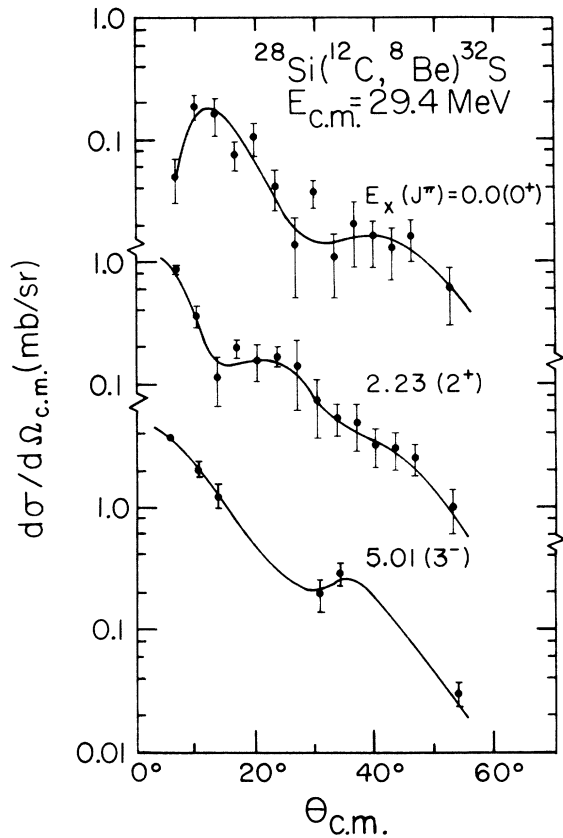


FIG. 8. Angular distributions for  $^{28}\text{Si}(^{12}\text{C}, ^8\text{Be})^{32}\text{S}$  at  $E_{c.m.} = 29.4$  MeV. The curves are drawn to connect data points pertaining to the same residual state.

action<sup>10</sup> measured over a more limited angular range. The smooth energy dependence of the cross sections observed at  $\theta_{lab} = 5^\circ$ , (see Fig. 9) favors a direct mechanism for the  $^{28}\text{Si}(^{12}\text{C}, ^8\text{Be})^{32}\text{S}$  reaction.

#### IV. SUMMARY

The  $^{16}\text{O}(^{16}\text{O}, ^8\text{Be})^{24}\text{Mg}^*$  reactions do not indicate any selectivity or direct reaction character. However, the  $^{12}\text{C}(^{12}\text{C}, ^8\text{Be})^{16}\text{O}^*$  reactions at  $E_{c.m.} = 16$  to 22 MeV seem to populate very selectively the members of the 4p-4h band in  $^{16}\text{O}$ . There is no measurable cross section for members of the 3p-3h band or the 8.87 MeV ( $2^-$ ) unnatural parity state. In the  $(^{12}\text{C}, ^8\text{Be})$  reactions, unnatural parity states are very weakly populated. This is consistent with a one-step reaction mechanism. In the  $^{12}\text{C}(^{12}\text{C}, ^8\text{Be})$  reaction, the 11.10 MeV ( $4^+$ ) state is populated with 5% to 25% of the cross section of the 10.34 MeV ( $4^+$ ) member of the 4p-4h band. In other four-particle transfer reactions, a stronger population of this 11.10 MeV state has been interpreted as evi-

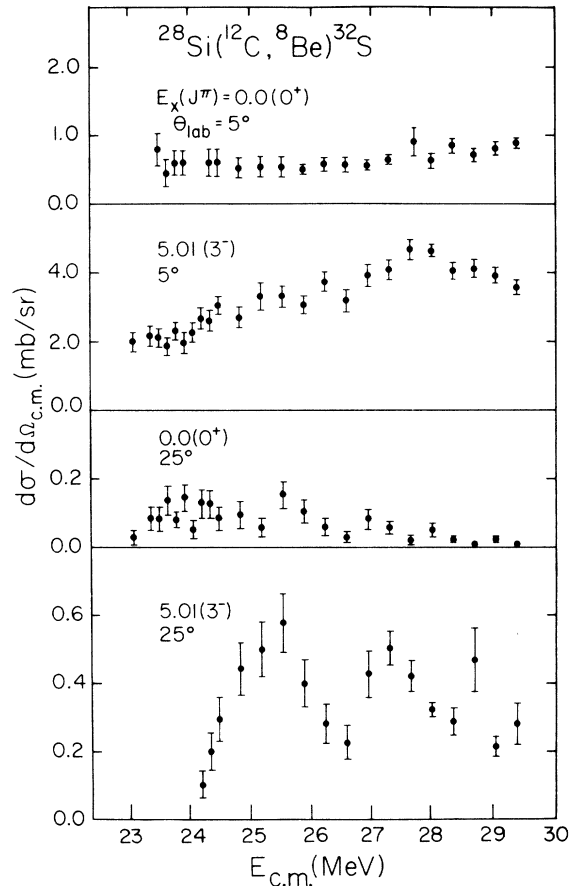


FIG. 9. Excitation functions for  $^{28}\text{Si}(^{12}\text{C}, ^8\text{Be})^{32}\text{S}$  leading to the ground state and the 5.01 ( $3^-$ ) excited state, measured at  $\theta_{lab} = 5^\circ$  and  $25^\circ$ .

dence for a two-step process.<sup>2</sup>

The selective population of the 4p-4h band in  $^{16}\text{O}$  is not entirely certain, because 1p-1h states could not be resolved from the  $0^+$  and  $2^+$  members of the 4p-4h band. Although theoretical calculations<sup>28</sup> indicate that the 6.13 MeV ( $3^-$ ), 1p-1h state could be excited from a mixing of 3p-3h components, the pure 3p-3h states were not observed in this reaction (see Fig. 3). The  $^{12}\text{C}_{g.s.} + \alpha$  overlap was calculated<sup>29</sup> to be quite large for the 11.25 MeV ( $0^+$ ), 2p-2h state in  $^{16}\text{O}$ , but this state was not observed in the  $^{12}\text{C}(^{12}\text{C}, ^8\text{Be})^{16}\text{O}^*$  reaction.

The state most strongly excited in the  $^{28}\text{Si}(^{12}\text{C}, ^8\text{Be})^{32}\text{S}^*$  reactions is the 5.01 MeV ( $3^-$ ) state. This is consistent with some  $(^6\text{Li}, d)$  reactions,<sup>9,11</sup> ( $^{16}\text{O}, ^{12}\text{C}$ ) results,<sup>26</sup> and the predicted enhancement of  $\alpha$ -particle transfer strength when the  $(sd)^3 (fp)^1$  configuration is formed.

The  $(^{12}\text{C}, ^8\text{Be})$  results presented resemble both the  $(^6\text{Li}, d)$  and the  $(^{16}\text{O}, ^{12}\text{C})$  reactions. These re-

actions appear to be somewhat direct in nature on the basis of selectivity. The selectivity and the smooth energy dependence of the  $^{28}\text{Si}(^{12}\text{C}, ^8\text{Be})$  cross sections favor a direct reaction interpretation although energy dependence in the  $^{12}\text{C}(^{12}\text{C}, ^8\text{Be})$ - $^{16}\text{O}$  results presented here and elsewhere is not consistent with a one-step direct transfer. Energy

dependence of the other reactions has not been reported.

The authors wish to acknowledge the assistance of Dr. Leon West and Dr. Gordon Morgan in this work, as well as the ion source development of Dr. Ken Chapman.

†Work supported in part by the National Science Foundation under Grants Nos. NSF-MPS-7503767 and NSF-GU-2612.

\*Present address: School of Physics, University of Minnesota, Minneapolis, Minnesota 55455.

‡Present address: Department of Physics, Florida A & M University, Tallahassee, Florida 32307.

<sup>1</sup>K. Bethge, in *Annual Review of Nuclear Science*, edited by E. Segrè, J. R. Grover, and H. P. Noyes (Annual Review, Inc., Palo Alto, 1970), p. 255.

<sup>2</sup>H. T. Fortune, in *Symposium on Heavy-Ion Transfer Reactions*, Vol. 1, Invited Papers, edited by J. P. Schiffer *et al.* (Informal Report No. PHY-1973B, Argonne National Laboratory, Illinois, March 1973), p. 287.

<sup>3</sup>K. Bethge, K. Meier-Ewert, K. Pfeiffer, and R. Bock, *Phys. Lett.* **24B**, 663 (1967).

<sup>4</sup>K. Meier-Ewert, K. Bethge, and K. O. Pfeiffer, *Nucl. Phys.* **A110**, 142 (1968).

<sup>5</sup>Pühlhoffer *et al.*, *Nucl. Phys.* **A147**, 258 (1970).

<sup>6</sup>M. L. Halbert, F. E. Durham, and A. Van der Woude, *Phys. Rev.* **162**, 899 (1967); L. R. Greenwood *et al.*, *Phys. Rev. C* **6**, 2112 (1972).

<sup>7</sup>R. Middleton *et al.*, *J. Phys. (Paris) Suppl.* **32**, C6 (1971).

<sup>8</sup>J. P. Draayer, H. E. Gove, J. P. Trentelman, N. Anantaraman, and R. M. DeVries, *Phys. Lett.* **53B**, 250 (1974).

<sup>9</sup>N. Al Jadir, D. J. Pullen, and R. Middleton, *Bull. Am. Phys. Soc.* **13**, 675 (1968).

<sup>10</sup>J. V. Maher, K. A. Erb, G. H. Wedberg, J. L. Ricci, and R. W. Miller, *Phys. Rev. Lett.* **29**, 291 (1972).

<sup>11</sup>R. A. Lindgren, J. P. Trentelman, N. Anantaraman, H. E. Gove, and F. C. Jundt, *Phys. Lett.* **49B**, 263 (1974).

<sup>12</sup>D. R. James *et al.*, *Nucl. Phys.* **A205**, 170 (1974).

<sup>13</sup>K. A. Eberhard *et al.*, University of Munich Accelerator Laboratory Annual Report, 1974 (unpublished), p. 84.

<sup>14</sup>G. R. Morgan, G. A. Norton, and N. R. Fletcher (unpublished).

<sup>15</sup>G. J. Wozniak, H. L. Harney, K. H. Wilcox, and Joseph Cerny, *Phys. Rev. Lett.* **28**, 1278 (1972).

<sup>16</sup>J. G. Cramer *et al.*, *Nucl. Instrum. Methods* **111**, 425 (1973); N. R. Fletcher *et al.*, *Bull. Am. Phys. Soc.* **19**, 427 (1974).

<sup>17</sup>F. Scheibling, Université Louis Pasteur, Strasbourg (private communication).

<sup>18</sup>W. Von Oertzen *et al.*, in *Nuclear Reactions Induced by Heavy Ions*, edited by R. Bock and W. R. Hering (North-Holland, Amsterdam and London, 1970), p. 156.

<sup>19</sup>J. C. Jacmart *et al.*, in *Nuclear Reactions Induced by Heavy Ions*, edited by R. Bock and W. R. Hering (North-Holland, Amsterdam and London, 1970), p. 128.

<sup>20</sup>K. D. Hilderbrand *et al.*, *Nucl. Phys.* **A157**, 297 (1970).

<sup>21</sup>M. S. Zisman, E. A. McClathchie, and B. G. Harvey, *Phys. Rev. C* **2**, 1271 (1970), and references therein.

<sup>22</sup>G. Bassani *et al.*, *Phys. Lett.* **30B**, 621 (1969).

<sup>23</sup>R. Wieland *et al.*, *Phys. Rev. C* **8**, 37 (1973).

<sup>24</sup>H. T. Fortune (private communication).

<sup>25</sup>N. R. Fletcher *et al.*, *Bull. Am. Phys. Soc.* **19**, 1076 (1974).

<sup>26</sup>J. Stettmeier *et al.*, in *Reactions Between Complex Ions*, edited by R. L. Robinson, F. K. McGowan, J. B. Ball, and J. Hamilton (North-Holland, Amsterdam and London, 1974), Vol. I, p. 84.

<sup>27</sup>C. Olmer *et al.*, in *Reactions Between Complex Ions* (see Ref. 26), Vol. I, p. 104.

<sup>28</sup>A. Arima, V. Gillet, and J. Ginocchio, *Phys. Rev. Lett.* **25**, 1043 (1970).

<sup>29</sup>M. Ichimura *et al.*, *Nucl. Phys.* **A204**, 225 (1973).